Journal of Structural Geology, Vol. 15, No. 12, pp. 1509 to 1512, 1993
Printed in Great Britain

0191-8141/93 $06.00+0.00

Brevia

SHORT NOTES

Fractal analysis of fracture patterns using the standard box-counting technique: valid and invalid methodologies

J. J. WALSH and J. WATTERSON

Department of Earth Sciences, University of Liverpool, P.O. Box 147, Liverpool L69 3BX, U.K.

(*Received* 10 *March* 1993; *accepted in revised form* 11 *May* 1993)

Abstract—On the basis of results of simple box-counting analysis, it has been suggested in several recent publications that natural fracture patterns are fractal. Fractal patterns are characterized by self-similarity of structure on a range of scales and provide straight-line distributions on box-counting plots. New analysis of a fracture pattern that provided the most convincing straight-line box-counting curve previously published, shows that the curve is non-linear and, therefore, that the fracture pattern is not fractal. Non-linear box-counting curves are also characteristic of other natural fracture patterns analysed but spurious linear curves can be obtained if the area analysed extends beyond the mapped area.

INTRODUCTION

THE CONCEPT that fault patterns show a degree of self-similarity over a wide range of scales has long been familiar to geologists (Tchalenko 1970). Self-similarity of structure is a characteristic of fractal geometries, in which any portion of the system is a scaled-down version of the whole (Mandelbrot 1983). A feature of a fractal geometry is that the relative numbers of large and small elements remain the same at all scales between the upper and lower fractal limits; the scaling relationship is described by the fractal dimension, which is simply derived from the power-law exponent on a plot of log size vs log cumulative number.

Recent work has shown that some elements of fault systems have fractal properties. For example, the populations of fault displacements (Kakimi 1980, Childs *et al.* 1990, Marrett & Allmendinger 1991, Walsh *et al.* 1991), fault trace lengths (Heffer & Bevan 1990, Yielding *et al.* 1992) and fault zone breccia clast sizes (Sammis *et al.* 1987) all provide power-law distributions. The morphologies of individual fault traces and of segmented faults also show fractal characteristics (Aviles *et al.* 1987, Power & Tullis 1991). The further claim has been made by some authors (Barton & Larsen 1985, Barton & Hsieh 1989, Hirata 1989) that fracture trace *patterns*, of fault and of joint arrays, also are fractal but others using the same technique claim that fracture trace patterns are not fractal (Odling 1992, Gillespie *et al.* in press). The purpose of this note is to reconcile these contradictory views by reference to results obtained by new analysis of a fracture trace map originally produced by Barton & Hsieh (1989) and interpreted by them as fractal.

ANALYSIS OF THE SPATIAL DISTRIBUTIONS OF FRACTURES

The conventional method of fractal analysis of fracture patterns is the box-counting technique (Barton & Larsen 1985), which is designed to measure the fractal dimension (or box dimension) of a fractal on a plane (Mandelbrot 1983, Falconer 1990). Square grids containing boxes of a given side length (d) are superimposed on a fracture pattern and the number of boxes (N_d) containing fractures is counted. This process is repeated for boxes of different sizes and the curve $\log d$ vs $\log N_d$ is plotted. Box-counting curves characteristically have limiting slopes of -2.0, for box sizes at which all boxes contain one or more fractures, and -1.0 for box sizes at which no box contains more than one fracture. Between these limiting slopes, the central segment of the box-counting curve is, for a fractal pattern, a straight line with slope $-D$ such that:

$$N_d \propto d^{-D},$$

where D is the fractal dimension of the pattern, with a value between 1.0 and 2.0. This central segment is the only part of the curve which is relevant to characterization of the pattern, as was pointed out by Barton & Hsieh (1989). For a non-fractal pattern the central segment is curved with the slope varying between -1.0 and -2.0. The method has obvious limitations with regard to characterization of fracture systems, e.g. the sizes of individual fractures are not taken into account. The method is most suited to arrays of intersecting fractures which fragment the rock surface into approximately equidimensional fragments, because the results

characterize the size distribution of the fragments rather than the fracture systematics.

There are differences in the methodologies employed by the various investigators who have applied the box-counting technique to fracture patterns. One difference concerns the objective identification of straight-line curves. It has been argued (Gillespie *et al.* in press) that regular curves have been mis-identified as straight lines, leading to the mistaken conclusion that the analysed patterns are fractal (e.g. Barton *et al.* 1988, Hirata 1989). This problem can be avoided by examining plots of box size vs curve slope over the whole range of box sizes, as shown below. Systematic changes in slope are easily identified in this way and most of the published box-counting curves which have been derived from fracture patterns have been concluded to be non-linear and the fracture patterns non-fractal (Gillespie *et al.* in press). However, notable exceptions are the box-counting curves (Barton & Hsieh 1989, fig. 9) derived from fracture maps of exposed pavements at Yucca Mountain, Nevada. Earlier curves derived from these fracture maps (Barton *et al.* 1988) are less straight. One of these maps (Pavement 1000 of Barton & Hsieh 1989, fig. 18, reproduced here as Fig. 1) and the box-counting curve derived from it (Barton & Hsieh 1989, fig. 9, reproduced here in Fig. 2) have been given wider currency as an example of a fractal fracture pattern (Turcotte 1992, figs. 4.4 and 4.5). The box-counting curve (Fig. 2) has a straight-line distribution over *ca* 2 orders of magnitude of box size, with a best-fit slope of *ca* −1.78.

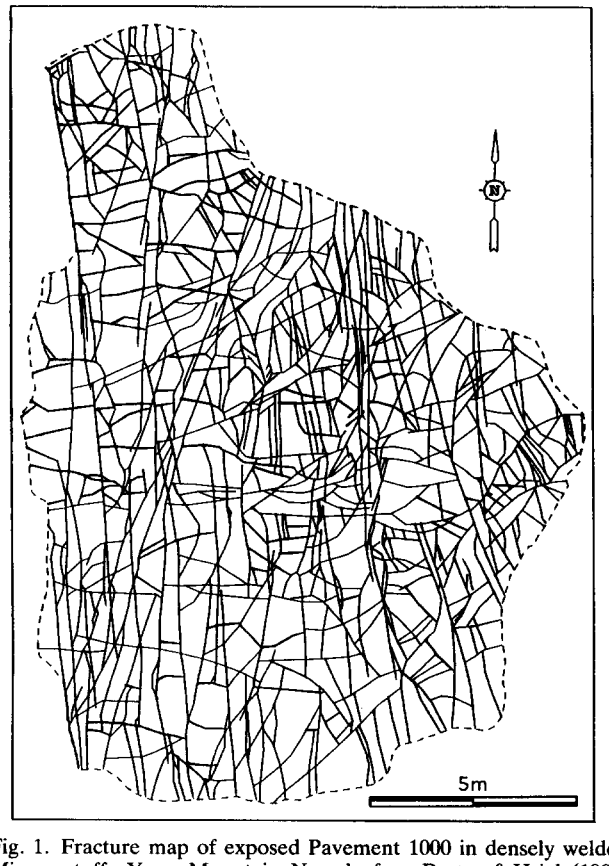

Fig. 1. Fracture map of exposed Pavement 1000 in densely welded Miocene tuffs, Yucca Mountain, Nevada, from Barton & Hsieh (1989, fig. 18).

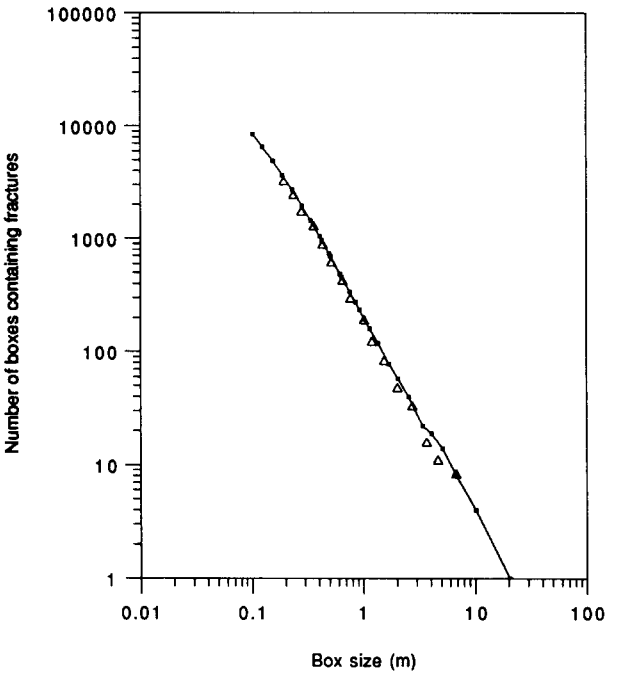

Fig. 2. Box-counting curves for fracture map in Fig. 1. Data points from Barton & Hsieh (1989) are shown as open triangles and were digitized from their fig. 9. The second curve (filled squares and solid line) is derived from an invalid box-counting run with a single initial box circumscribing the fracture map (see also Figs. 3 and 4).

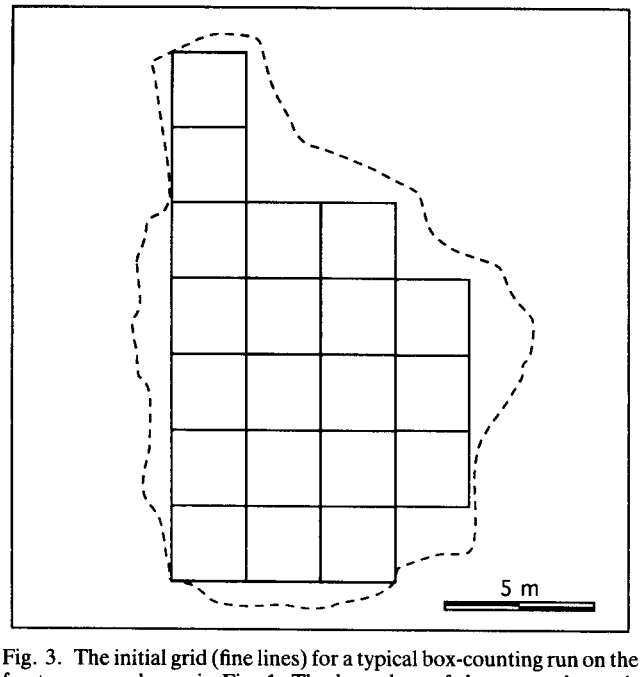

Fig. 3. The initial grid (fine lines) for a typical box-counting run on the fracture map shown in Fig. 1. The boundary of the mapped area is shown by the broken line. Also shown is the single circumscribing box (heavy line) used as the single initial box for the invalid box-counting run giving rise to a power-law curve (see Fig. 2).

We have carried out our own box-counting analysis of the map and attempted to reproduce the straight-line curve. The map analysed was digitized from Barton & Hsieh (1989, fig. 18) using a standard industry mapping package. Since the outline of the mapped fracture pattern is irregular it is not possible to include the entire map in a box-counting analysis. The initial box size, the

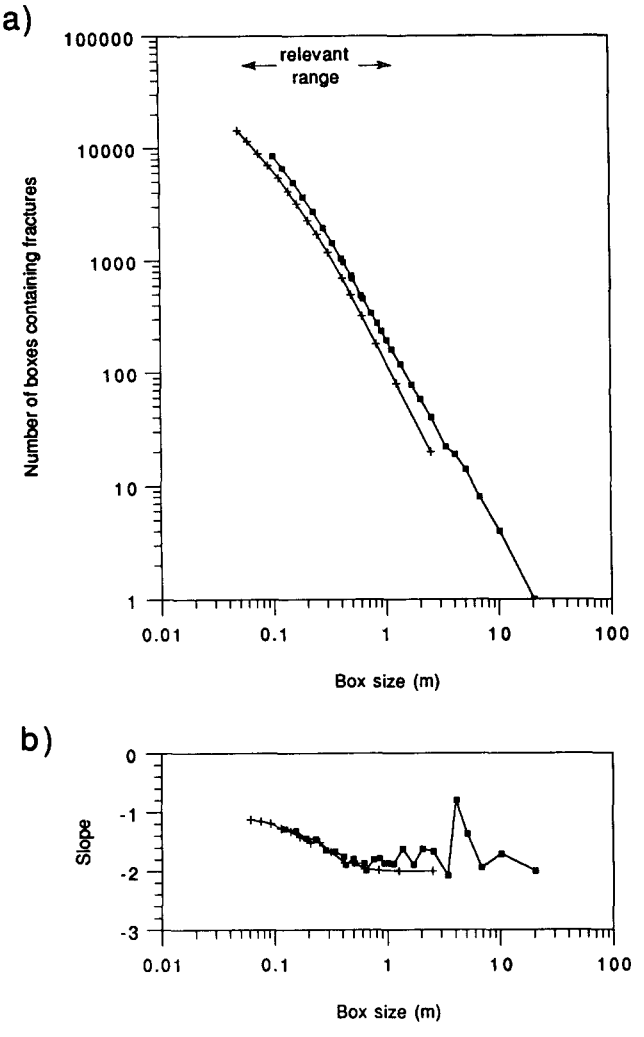

Fig. 4. (a) Box-counting results for the fracture map shown in Fig. 1 using: (i) the multi-box initial grid shown in Fig. 3 (crosses); and (ii) the single circumscribing initial box shown in Fig. 3 (filled squares). Regression analysis of the curves (incorporating all of the data points shown) provides the following 'fractal dimensions' (D) and correlation coefficients (r): $D = 1.67$ and $r = 0.994$ for curve (i) and $D = 1.77$ and $r = 0.999$ for curve (ii). (b) Box size vs slope plots for each of the curves in (a). Slope values are those calculated between successive pairs of adjacent data points.

position of the origin and the orientation of the box-counting grid relative to the fracture map determine what proportion and which parts of the map are analysed by a particular box-counting run (see Fig. 3). A box-counting curve for one starting array of boxes is shown in Fig. 4(a); curves generated using a range of initial box arrays have similar slopes and curvatures but vary in position. Even though regression lines for these curves have high correlation coefficients (0.994 for curve i shown in Fig. 4a) they are, nevertheless, not straight but are systematically curved and without a power-law central segment. Our analysis of the Pavement 100 fracture map of Barton & Hsieh (1989) gives similar results. High correlation coefficients are mainly due to the ranking of box numbers which limits the scatter about any curve and regression analysis is not therefore well suited to discriminating between straight and curved box-counting curves.

The curvature is illustrated by a plot of the slopes between adjacent data points on an individual box-counting curve (Fig. 4b). The gradual change in slope from -2.0 to -1.0 is characteristic of all curves generated by this technique for this fracture pattern. A slope of -2.0 occurs at box sizes greater than the maximum unfractured block, or fragment, size and a slope approaching -1.0 at the minimum box size analysed. At large box sizes the slope is measuring the degree of plane-filling of the fracture pattern and at small box sizes the slope is, in the limit, measuring the roughness of individual fractures. The different positions of other box-counting curves for this fracture pattern are largely a function of the differences in total fracture trace length within the areas covered by the initial box array in each box-counting run. Only with rectilinear and orthogonal map boundaries is it possible to include the whole map within the initial array of boxes without including unmapped ground.

However, if a box-counting curve is constructed for this map using a single initial box which circumscribes the fracture map, the resulting box-counting curve is straight over much of its length (from 20 m to <40 cm for curve ii of Figs. 2 and 4), with a slope of *ca* -1.8 (Fig. 4b) and is approximately coincident with that derived by Barton & Hsieh (1989); at similar scale ranges the box-counting curve for the multi-box initial grid has a slope of *ca* -2.0. Note that projections of both curves intersect the abscissa at a box size of *ca* 20 m, which is the size of a circumscribing box. The abrupt offset of our curve at large box sizes (*ca* 4 m) is due to the effects of the long straight left-hand boundary of the map being parallel to the box-counting grid. Our relatively straight box-counting curve has little geological significance since it incorporates the scaling properties both of the unmapped ground, external to the map but within the single initial box, and of the mapped fracture pattern; we believe the same to be true of the previously published curve. More importantly, because the straight line distribution extends to box sizes which are significantly greater than the maximum fragment size in the fracture pattern, which is *ca* 1 m^2, the previously published curve can have only a tenuous relationship with the scaling properties of the fracture pattern. A box-counting curve should extend to box sizes comparable with the sizes of the smallest fragments in the pattern because it is in this range that the curvature is most marked (see Fig. 4). The box-size range relevant to the fracture pattern is indicated in Fig. 4(a). The previously published straight-line curve is therefore not a valid representation of the analysed fracture pattern. As the curves derived using a valid methodology clearly are non-linear it is concluded that the fracture pattern is not fractal.

DISCUSSION AND CONCLUSIONS

Box-counting analysis of a fracture pattern previously reported to be fractal provides a non-power-law distribution indicating a non-fractal geometry. Gillespie *et al.* (in press) have shown that other fracture maps also do

not provide power-law box counting curves. A fracture pattern incorporates many different attributes such as orientation distribution, size population and fracture trace geometry. It is therefore unlikely that natural fracture patterns could, for all but the simplest of cases, be characterized by a single fractal dimension over a significant scale range.

The example illustrated highlights the importance of applying a strict methodology to box-counting analysis. Unmapped ground outwith the fracture map must not be included in the area analysed; the fact that a box-counting run need not start with a single initial box makes this condition less restrictive than would otherwise be the case. The exclusion of unmapped ground will usually require that some parts of the fracture pattern, particularly those close to the map boundary, be omitted from a box-counting run. Several runs should be made to test the sensitivity of the results to exclusion of different parts of the map. There is a trade-off between maximizing the area analysed and maximizing the size of the initial boxes. The box-counting should be performed over as wide a range of box sizes as is possible but the relevant part of the curve is that corresponding to box sizes between those of the largest and smallest fragments or fracture spacings. Beyond these limits the slope of the curve tends to -2.0 and -1.0. Analysis over the widest possible range of box sizes, i.e. beyond the valid range, is recommended in order to track these slope changes more precisely and to define the valid range objectively. Linear regression should be carried out only on those parts of the curve within the valid range. Regression lines with high correlation coefficients are not, however, diagnostic of power-law curves which are best identified with plots of box size vs slope.

Acknowledgements—Steve Easton, Dan Ellis, Colin Howard, Paul Gillespie and Phillipa Mason of the Fault Analysis Group at Liverpool are thanked for their help in the processing and analysis of fracture patterns. This work was carried out as part of a project funded by the E.C. JOULE Programme (contract JOUF-0036-C).

REFERENCES

Aviles, C. A., Scholz, C. A. & Boatwright, J. 1987. Fractal analysis applied to characteristic segments of the San Andreas Fault. *J. geophys. Res.* **92**, 331–334.

Barton, C. C. & Larsen, E. 1985. Fractal geometry of two-dimensional fracture networks at Yucca Mountain, Southwest Nevada. In: *Fundamentals of Rock Joints* (edited by Stephannson, O.). Proceedings of the International Symposium on Fundamentals of Rock Joints, Bjorkkliden, Sweden, 77–84.

Barton, C. C., Larsen, E., Page, W. R. & Howard, T. M. 1988. Characterizing fractured rock for fluid flow, geomechanical, and paleostress modelling: methods and preliminary results from Yucca Mountain, Nevada (methods for parameterizing fracture characteristics at the scale of large outcrops). *Bull. U.S. geol. Surv.*, March 3.

Barton, C. C. & Hsieh, P. A. 1989. *Physical and Hydrologic-flow Properties of Fractures*. 28th International Geological Congress Field Trip Guidebook T385, American Geophysical Union, Washington, DC.

Childs, C., Walsh, J. J. & Watterson, J. 1990. A method for estimation of the density of fault displacements below the limits of seismic resolution in reservoir formations. In: *North Sea Oil and Gas Reservoirs*—II (edited by Buller, A. T., Berg, E., Hjelmeland, O., Kleppe, J., Torsaeter, O. & Aasen, J. O.). Graham & Trotman, London, 309–318.

Falconer, K. 1990. *Fractal Geometry: Mathematical Foundations and Applications*. Wiley, Chichester.

Gillespie, P., Howard, C. B., Walsh, J. J. & Watterson, J. In press. Measurement and characterisation of spatial distributions of fractures. *Tectonophysics*.

Heffer, K. J. & Bevan, T. G. 1990. Scaling relationships in natural fractures—Data, theory and applications. *Soc. Petrol. Engrs*, Reprint No. **20981**, 1–12.

Hirata, T. 1989. Fractal dimension of fault systems in Japan: fractal structure in rock fracture geometry at various scales. *Pure & Appl. Geophys.* **131**, 157–169.

Kakimi, T. 1980. Magnitude-frequency relation for displacement of minor faults and its significance in crustal deformation. *Bull. geol. Surv. Jap.* **31**, 467–487.

Mandelbrot, B. B. 1983. *The Fractal Geometry of Nature*. W. H. Freeman, New York.

Marrett, R. & Allmendinger, R. W. 1991. Estimates of strain due to brittle faulting: sampling of fault populations. *J. Struct. Geol.* **13**, 735–738.

Odling, N. E. 1992. Network properties of a two-dimensional natural fracture pattern. *Pure & Appl. Geophys.* **138**, 95–114.

Power, W. L. & Tullis, T. E. 1991. Euclidean and fractal models for the description of rock surface roughness. *J. geophys. Res.* **96**, 415–424.

Sammis, C., King, G. & Biegel, R. 1987. The kinematics of gouge deformation. *Pure & Appl. Geophys.* **125**, 777–812.

Tchalenko, J. S. 1970. Similarities between shear zones of different magnitudes. *Bull. geol. Soc. Am.* **81**, 1625–1640.

Turcotte, D. L. 1992. *Fractals and Chaos in Geology and Geophysics*. Cambridge University Press, Cambridge.

Walsh, J. J., Watterson, J. & Yielding, G. 1991. The importance of small-scale faulting in regional extension. *Nature* **351**, 391–393.

Yielding, G., Walsh, J. J. & Watterson, J. 1992. The prediction of small-scale faulting in reservoirs. *First Break* **10**, 449–460.